DOI: 10.1002/ejoc.200800187

Nucleohomolytic Substitution at Boron: A Computational Approach

Claudio Carra[a] and Juan C. Scaiano*[a]

Keywords: Boron / Nucleophilic substitution / Density functional calculations / Radicals

A theoretical investigation is reported on the reaction mechanism for oxygen-centered radical attack on alkyl- and arylborane substrates. The model reveals how the mechanism, traditionally considered as a S_H2 reaction, involves instead nucleophilic attack of the oxygen lone pair on the empty boron p orbital. The single electron on the oxygen is not directly involved in the process, however, as a result of a stereoelectronic effect: the bond aligned with the SOMO orbital is deactivated and the corresponding ligand leaves promptly as a radical species. The overall mechanism can be described as a *nucleohomolytic reaction* that shares many characteristics with conventional nucleophilic substitution.

Introduction

Organometallic compounds of group 13 elements show high chemical reactivity, which is normally attributed to electron deficiency of the empty orbital on the central atom.[1] Their reactivity as strong Lewis acids is a well-established characteristic for these elements.[2] It has been long recognized that the homolytic substitution (S_H2) reactions can occur, often with high rate constants, on a metallic center of an organometallic system, according to the general reaction scheme:[3]

$$X^{\cdot} + MR_n \rightarrow XMR_{n-1} + R^{\cdot}$$

Bimolecular homolytic attack by free radicals at metal centers have been known for almost half a century; these processes provided an example of the behavior of free radicals, and a great variety of organometallic reactions of this type have been reported.[3–5] Among these, reactions at boron centers were extensively studied largely three decades ago,[4,5] and recently reviewed.[6] In a typical "S_H2" reaction, an oxygen radical may displace an alkyl radical, as shown in Reaction (1).[3,4]

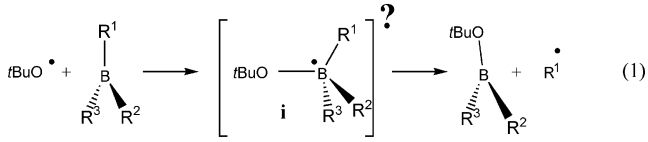

(1)

1: R¹, R², R³ = Me **2:** R¹, R², R³ = *t*Bu **3:** R¹, R², R³ = vinyl **4:** R¹, R² = Me, R³ = Ph **5:** R¹, R², R³ = Ph

Species **i** has proven elusive and has never been detected when R is aliphatic, and it has only been detected in the case of **5** for aromatic systems; the intermediate was detected by using laser flash photolysis techniques.[7] Reaction (1) has normally been viewed as an attack of the single occupied orbital of the oxygen on the vacant p orbital of the boron. In this work, we show that this well-established interpretation requires revision. Reaction (1) is in fact a close relative of nucleophilic bimolecular substitution (S_N2) where the attack involves primarily the oxygen lone pair. Further, our calculations reveal that no tetravalent intermediate is expected in the case of aliphatic systems, but its involvement is expected only in aromatic systems. The fact that these reactions are frequently controlled by steric rather than thermodynamic effects can be readily rationalized given the nucleophilic-like nature of the transition state.[1]

Theoretical Methods

All calculations were performed by using the Gaussian 03 package.[8] A comparative study was carried out by locating the stationary points on the potential energy surface (PES) by using different hybrid density functional methods (B3LYP,[9] B3PW91,[10] BHandH,[11] MPW1PW9)[12] with different basis sets (6-31G*,[13] 6-31+G**,[13] 6-311+G*,[14] cc-pVDZ[15]). In the models used to describe the chemical reaction path, the *tert*-butyl substituent in the *tert*-butoxyl radical was replaced with a methyl group.

In order to evaluate the role of the steric hindrance of the *tert*-butyl moiety, the system studied experimentally was also considered and studied at the same level of theory. We attempted to use different levels of theory, such as MP2[16] and high-level mixed methods (G2[17] and G3[18]) but we could not get the SCF convergence due to high-spin contamination of the wavefunction of the systems containing phenyl ligands. The other post Hartree–Fock methods were not considered because they are too demanding for our computer resources. As a consequence for our investigation we limit the use to only DFT methods, which can, however,

[a] Department of Chemistry, University of Ottawa, Ottawa, Ontario K1N 6N5, Canada
Fax: +1-613-562-5633
E-mail: tito@photo.chem.uottawa.ca

give reliable results if combined with appropriate basis sets.[19]

The analytical second-order derivative of the energy with respect to the nuclear position was performed to determine the nature of the stationary point considered. Zero-point vibrational energies were calculated by using the harmonic approximation. The thermodynamic properties were evaluated with the harmonic/oscillator, rigid rotator implemented in Gaussian 03. The atomic charges were calculated with the natural population analysis.[20] In order to depict in more detail the stereoelectronic effect, the natural bond orbital (NBO)[21] method, implemented in Gaussian 03 as NBO 3.0.G,[20–22] was used. The graphical representation of the optimized structures and the corresponding isosurfaces are plotted with Molekel 4.[23]

Results and Discussion

The first case examined was attack of the methoxyl radical on trimethylborane. The corresponding intermediate **1i** could not be located by B3LYP or MP2, because for the optimized B–O distance, there is spontaneous loss of a methyl radical. In order to determine the potential energy profile of the entire reaction, a relaxed scan of the O–B distance was performed by B3LYP/6-31G*. The bond length, initially set at 3 Å, was reduced by 0.1 Å to the optimal value of 1.366 Å. One of the methyl fragments spontaneously leaves as $CH_3^{\cdot}$ once the B–O bond length is reduced to 1.49 Å, excluding the possibility of a barrier for the B–C bond scission. The overall reaction is exothermic by 23.1 kcal/mol. In Figure 1 we show the spin isodensity surface and the lone pair for two optimized structures with a constrained B–O distance of 2.5 Å and 1.7 Å, respectively. During the approach of the methoxyl radical, the spin distribution, fully localized on the $MeO^{\cdot}$ for a distance of 2.5 Å (Figure 1a), increases its delocalization in the C–B bond positioned almost orthogonally to the axis of the singly occupied molecular orbital (SOMO) of the oxygen atom (Figure 1c).

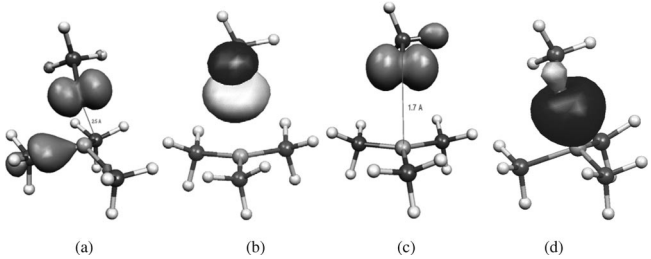

Figure 1. Attack of methoxyl radical on trimethylborane: spin density of **1** for an optimized structure with a fixed O–B distance of 2.5 Å (a) and 1.7 Å (c). The corresponding lone pair MO of the oxygen atom (b) with its increase in σ character (d).

On the same constrained geometries the orientation of the lone pair (Figure 1a,c) towards the boron center excludes a pure radical attack as a mechanism for S_H2 reactions.

To gather more information on the reaction mechanism, we considered the effect of different substituents on the boron center. The replacement of the methyl group with a *tert*-butyl group, **2i**, leaves the chemical behavior unmodified. The loss of the alkyl radical is always barrierless and energetically favorable. Given that the S_H2 reaction is highly exothermic, to increase the possibilities to have a true intermediate, it is necessary to stabilize the reactant and/or destabilize the product.

Substituents having π bonds conjugated with the boron atom are a suitable choice for this purpose: here unsaturation is anticipated to stabilize the tetravalent intermediate by delocalizing the radical center and destabilize the product by giving a highly unstable σ sp^2 radical. The first substrate examined was trivinylborane (**3**). The corresponding methoxy intermediate **3i** was found and fully optimized by B3LYP/6-31G* (Figure 2a).

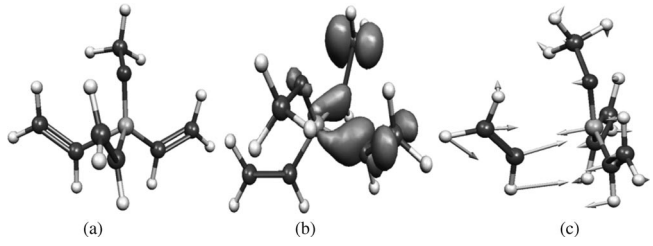

Figure 2. Geometry of **3i** (a), the corresponding spin density (b), and the TS to the C–B bond scission showing the components of the negative eigenvalue (arrows; c).

Its spin density (Figure 2b) is almost completely delocalized over two vinyl substituents, with a low spin density on the oxygen atom. There is, however, a substantial difference in the spin distribution on the two vinyl moieties. In the case of the vinyl group orthogonal to the methyl oxygen axis, the spin density is mostly centered in the C–B bond, whereas on the adjacent substituent, almost aligned to the methoxyl group, the spin localization is dominant on the terminal p orbital of the vinyl CH_2 group.

The bond lengths are altered by the distribution of the spin density. When it is mostly localized on the σ(B–C) bond, the bond becomes stretched (1.729 Å) and ready to cleave. However, when the spin density is more localized in the CH_2 terminal, the elongation of the C–B bond is less pronounced (1.615 Å) and much closer to the remaining C–B bond whose length is 1.591 Å.

The vinyl loss reaction occurs with a barrier of 3.54 kcal/mol, calculated by B3LYP/6-31G*, and the corresponding transition state was located and fully characterized with the analysis of the components of the negative eigenvalue of the analytical Hessian (Figure 2c). The cleaving bond is thus highly elongated (2.318 Å), and the boron center gains a strong sp^2 character, as shown by the substantial increase in the planarity of the remaining substituents.

The next step of the study was conducted to understand whether aromatic ligands may play a different role in the S_H2 process. Interestingly, the presence of only one phenyl fragment, **4**, does not stabilize **i** enough, and further, no TS could be located. The attacking group, while approaching

the substrate, rotates along the O–B axis, independently from the initial guess, toward a suitable conformation that can lead to the loss of the methyl radical.

The only case in which an intermediate was located by DFT was for triphenylborane (**5i**), which is known to have a detectable intermediate[7] (Figure 3a). The geometry at the boron center is a distorted tetrahedron, with a trigonal pyramidal component, due to the slightly stretched bond of the leaving phenyl group.

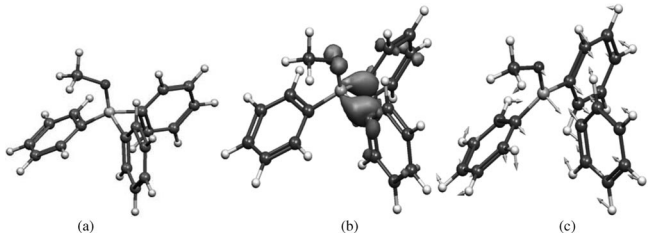

Figure 3. Attack of methoxyl radical on triphenylborane: geometry of **i** (a), the corresponding spin density (gray surface; b), and the TS for the C–B bond scission showing the component of the negative eigenvalue (c).

The correlation between the spin density and the length of the bonds involved in the reaction for **5i** is similar to the previous case of **3i**. In Figure 3b, the spin density of **5i** is highly localized in the σ(C–B) of the phenyl group almost orthogonal to the methoxyl moiety, that is, the leaving group. The phenyl substituent almost planar to the methoxyl substituent has the spin localized mostly on the π system. The C–B bond length for the leaving group is 1.731 Å, revealing significant bond deactivation, whereas the adjacent group has a higher π spin distribution and a shorter bond length (1.655 Å). Both values are larger than the remaining B–C bond (1.613 Å). The negative eigenvalue of the transition state (Figure 3c) is dominated by a complex series of vectors that describe two main distinct motions. The first corresponds to the B–C bond scission and the second shows an increase in the planarity of the boron center in MeOBPh, which is the product of reaction.

Several hybrid DFT methods are available,[24] and the recent ones show increased agreement with the prediction of reaction barriers.[25] Despite the improvement in the accuracy of the calculated values, there are still discrepancies in the results depending on the functional and basis sets used. Consequently, different methods were used to predict the activation energy.

Initially, the barrier for bond cleavage was calculated with different DFT methods (B3LYP, MPW1PW91, B3PW91, and BHandH) by using the 6-31G* basis sets. The last functional predicted a spontaneous dissociation of the phenyl radical. In all cases, the value of the activation energies is low (3.3 and 3.5 kcal/mol by B3PW91 and MPW1PW91, respectively, and only 1.9 kcal/mol by B3LYP). The reaction is exothermic only by B3LYP calculations (–1.4 kcal/mol), whereas calculations by MPW1PW9 and B3PW91 indicate that the product is endothermic by 1.9 and 2.0 kcal/mol, respectively.

To calculate the barrier of phenyl loss in a more quantitative way, different basis sets (6-31G*, 6-31+G**, cc-pVDZ, and 6-311+G*) were used with the functionals mentioned above. The activation energies and the B–C and B–O distances for **5i** and for transition state **5i**‡ are shown in Table 1.

In all cases, for a given method, the $\Delta E^{\ddagger}$ and $\Delta G^{\ddagger}$ values are very similar, with a fluctuation of less than 1 kcal/mol. A change in the basis set used only modestly influences the values calculated. A moderate decrease in the energies occurs by introducing diffuse functions and switching to a more extended basis set. The major difference is, however, due the functional used; B3LYP predicts the lowest barrier, with an average value among the different basis sets of 1.8 kcal/mol for $\Delta E^{\ddagger}$ and 1.5 kcal/mol for $\Delta G^{\ddagger}$. The use of B3PW91 and MPW1PW91 functionals gave a higher estimate of $\Delta E^{\ddagger}$, with an average value of 3.5 kcal/mol. For the reactant, the distances considered are almost unaffected by changing the basis set; however, there is a constant decrease in the length of the B–O bond from B3LYP to B3PW91 and MPW1PW91, changing from a average value of 1.431 to 1.423 Å. The B–C distances are nearly constant between B3PW91 and MPW1, with a value of 1.716 Å, which is shorter than the corresponding distance calculated by B3LYP (1.733 Å). At the transition state, the two bond lengths are more sensitive to the functionals, but no specific behavior seems to be followed except for the B–C distance, which is shorter by B3LYP.

To evaluate the effect of the steric hindrance on the barrier of activation, attack of the *tert*-butoxyl radical on triphenylborane was also considered. The results are summarized in Table 2. The change in the energetics with respect to **5i** is minor and less than 1 kcal/mol. In general, the B3LYP energy barriers are increased by ca. 0.5 kcal/mol,

Table 1. $\Delta E^{\ddagger}$ and $\Delta G^{\ddagger}$ energies of activation (in kcal/mol) of **5i**‡, B–C distance of the leaving group (in Å) of **5i** and **5i**‡.

		B3LYP				B3PW91				MPW1PW91			
Basis set		$\Delta E^{\ddagger}$	$\Delta G^{\ddagger}$	*d*(B–O)	*d*(B–C)	$\Delta E^{\ddagger}$	$\Delta G^{\ddagger}$	*d*(B–O)	*d*(B–C)	$\Delta E^{\ddagger}$	$\Delta G^{\ddagger}$	*d*(B–O)	*d*(B–C)
6-31G*	**5i**‡	1.9	1.8	1.392	2.178	3.5	3.6	1.383	2.309	3.3	3.1	1.380	2.284
	5i	–	–	1.430	1.731	–	–	1.426	1.714	–	–	1.422	1.714
6-31+G**	**5i**‡	1.8	1.3	1.394	2.154	3.4	3.1	1.384	2.287	3.2	2.7	1.382	2.257
	5i	–	–	1.431	1.733	–	–	1.427	1.716	–	–	1.423	1.716
cc-dDZ	**5i**‡	1.8	1.5	1.395	2.168	3.5	3.4	1.383	2.284	3.6	2.8	1.383	2.284
	5i	–	–	1.433	1.736	–	–	1.429	1.716	–	–	1.426	1.717
6-311+G*	**5i**‡	1.6	1.4	1.393	2.138	3.4	2.6	1.382	2.291	3.1	2.2	1.380	2.270
	5i	–	–	1.429	1.735	–	–	1.425	1.716	–	–	1.422	1.714

whereas the corresponding free energy is reduced by ca. 0.3 kcal/mol, independent of the basis set used. The B3PW91 functional behaves similarly to B3LYP. MPW1PW91 gives more consistent results and there are no significant differences with respect to the data of **5i**.

Table 2. $\Delta E^{\ddagger}$ and $\Delta G^{\ddagger}$ energies of activation (in kcal/mol) for the *tert*-butoxyl radical reaction.

	B3LYP		B3PW91		MPW1PW91	
Basis set	$\Delta E^{\ddagger}$	$\Delta G^{\ddagger}$	$\Delta E^{\ddagger}$	$\Delta G^{\ddagger}$	$\Delta E^{\ddagger}$	$\Delta G^{\ddagger}$
6-31G*	2.3	1.5	4.0	2.9	3.9	2.8
6-31+G**	2.0	1.3	3.7	2.6	3.6	2.6
cc-dDZ	2.1	1.4	3.9	2.8	3.7	2.7
6-311+G*	1.6	1.0	3.4	2.4	3.4	2.2

Beyond providing a quantitative description of the phenomena, we are interested in understanding in more detail the mechanism of bond breaking during the homolytic substitution at the boron center. With this objective in mind, we performed a study based on NBO analysis. The theory, developed by Weinhold and coauthors,[21] can be used to unravel the importance of the hyperconjugative interactions in chemical phenomena.

Because the spin density of **1i** is localized on the oxygen atom and on the cleaving bond, the orbitals considered in the NBO analysis are the σ and σ* of the leaving methyl group and the one-center singly occupied natural bond orbital of the oxygen [$SBO_{(O)}$; Figure 4, **I**–**III**]. For analogy, the equivalent orbitals are shown for **5i** (Figure 4, **I′**–**III′**).

In view of the fact that the interacting orbital of the oxygen atom has only one electron, two distinct possibly dominant hyperconjugative effects have to be considered to reduce the energy of the system by donor–acceptor interactions. Even though both occur at the same time, they can be described separately. The vicinal $SBO_{(O)} \rightarrow \sigma^*_{(B-C)}$ interaction stabilizes the singly occupied orbital. The resulting $SBO_{(O)}$ is closer in energy to the $\sigma_{(B-C)}$ enhancing the stabilization energy due to the $\sigma_{(BC)} \rightarrow SBO_{(O)}$ interaction (Figure 5a). The isosurfaces, which depict the donor→acceptor

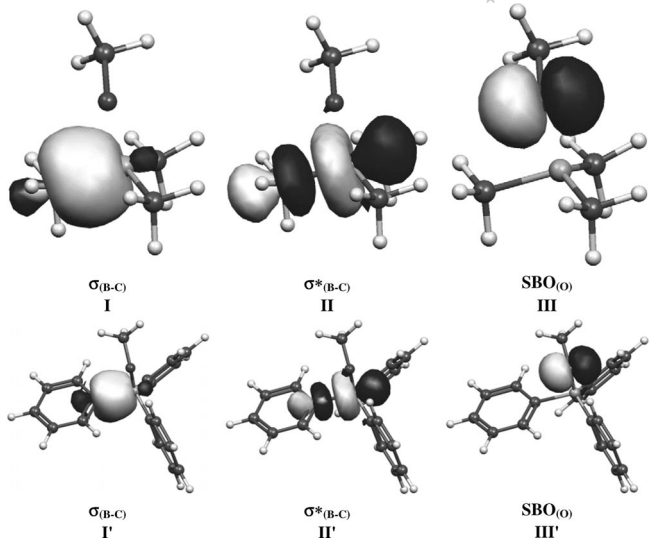

Figure 4. NBOs directly involved in the stereoelectronic effect for systems **1i** and **5i**. The σ and σ* of the cleaving B–C bond (**I** and **II**; **I′** and **II′** for **5**) and the single occupied natural bond orbital of the oxygen [$SBO_{(O)}$ **III**; **III′** for **5**].

interaction, are shown in Figure 5, where **I** is the sum of the $SBO_{(O)}$ and σ* and **II** is the sum of σ and $SBO_{(O)}$ for system **1i** (**I′** and **II′** are the corresponding surfaces for **5i**). This effect increases the weight of the resonance structure with the radical localized on the leaving group (Figure 5b), giving as a final result a weakening of the cleaving bond. To maximize the stabilization energy by hyperconjugation, the methoxyl moiety was positioned to have the biggest overlap between $SBO_{(O)}$ with the σ and σ* of the leaving group.

When the methyl groups at boron are replaced with phenyl substituents, as in **5i**, a series of interactions occur. In the presence of the aromatic rings, the stereoelectronic effect is extended where the π systems are positioned in an effective way to maximize the overlap with the $SBO_{(O)}$, that is, the conjugation effect becomes important, consistently

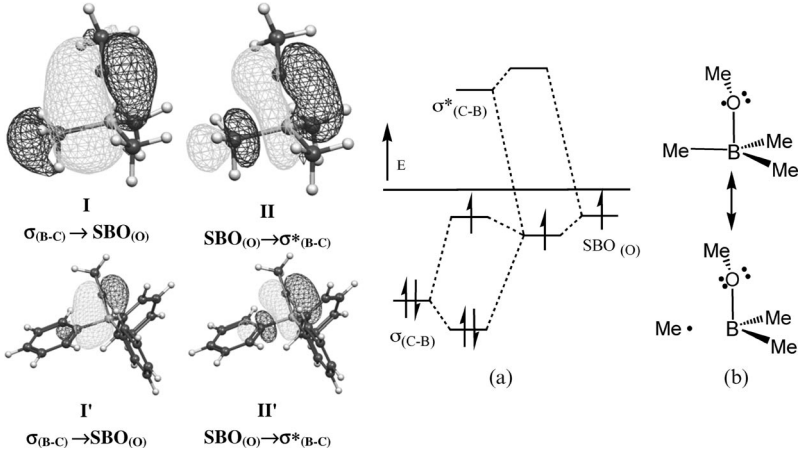

Figure 5. The hyperconjugative interaction $\sigma_{(B-C)} \rightarrow SBO_{(O)}$ and $SBO_{(O)} \rightarrow \sigma^*_{(B-C)}$ are described by the sum of the isosurfaces of the corresponding NBOs for models system **1i**, **I**, and **II**, and the real one **5i**, **I′**, and **II′**. Energy changes due to hyperconjugative effects for model system **1i** (a) and modification of the weight of the two resonance structures (b).

with the extensive delocalization of the spin density. The additional conjugative effect due to the conjugate π system, however, does not change qualitatively the overall process.

The data relative to bond orders (BO) gathered from NBO analysis is consistent with stereoelectronic effect considerations. For **1i**, the B–O bond reveals a low covalent character, with a BO of only 0.55, and this result is consistent with the long B–O distance constrained to 1.7 Å. The leaving methyl group has a BO value of 0.74, which underlies the strong deactivation of the σ bond. The $SBO_{(O)}$ also has a low population, with an occupancy number of 0.84. The remaining bonds have a much higher BO (0.90 and 0.92) and are almost unaffected by hyperconjugation with $SBO_{(O)}$ (Figure 6a). When the boron is substituted with phenyl rings, the population is modified by the conjugative effect of the π system. The BO of the leaving phenyl group still has a small value of 0.71, as the adjacent σ′ bond with a higher value of 0.78 (Figure 6b). The vicinal σ′(BC) bond, moreover, also plays a role with a hyperconjugation interaction with the breaking σ bond, confirmed by the small CBC angle of 87.1° compared with 109.1° in **1i**. The remaining phenyl moiety has a BO of 0.87 the highest value of all the boron bonds. The delocalization of the spin density in the aromatic rings allows the methoxyl group to be much closer to the boron before the dissociation than in the case of **1i**. The optimized distance is 1.430 Å, and the resulting bond has a strong covalent character with a BO of 0.78. With methyl substituents, where the conjugative effect is absent, the deactivation of the bond is already substantial at the fixed distance of 1.7 Å, preventing, as the attacking group approaches, any chance to isolate the intermediate.

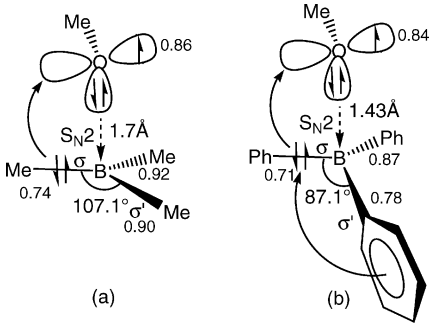

Figure 6. General mechanism for methoxyl radical attack to trimethylborane (a) and triphenylborane (b). The BO and the occupancy of $SBO_{(O)}$ is reported for both structures.

The discussion on the electron density and on the hyperconjugative effect is consistent with a change in the atomic charges during the process. Initially, in **1**, when the methoxyl group is set at 3.0 Å from the boron center, the Mulliken charges of the oxygen, boron, and leaving methyl fragment are –0.279, 0.489, and –0.175, respectively. At a closer distance of 1.7 Å, the atomic charges are significantly different. The oxygen atom is more negative, with a charge of –0.427, the boron atom more positive at 0.538, and the methyl fragment is at 0.012, which is almost neutral, as expected for the product of dissociation. The absence of spin density on boron rules out the assignment of the mechanism as a pure S_H2 reaction, where the SOMO would be oriented toward the reactive center.

The overall conclusion is that the initial attack at boron has nucleophilic rather than homolytic character and is consistent with the recent work by Wood,[26] which shows that water is a good hydrogen donor when coordinated with B^{III} compounds. Indeed, as illustrated in Figure 7, hydrogen abstraction from coordinated water can be viewed as occurring on the same hypersurface as attack of the hydroxyl radicals on boron.

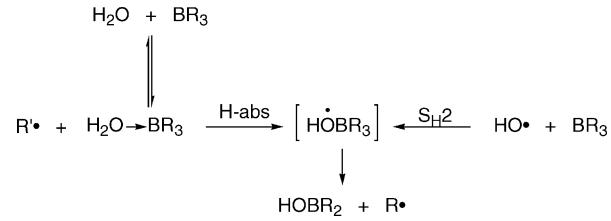

Figure 7. Hydrogen abstraction from coordinated water.

A similar mechanism is hypothesized for pentacoordinate phosphorus species where there is an unexpected reduction in the activation energy.[27] Similarly, for a Si center reaction, the central barrier is highly reduced from the carbon center to a Si center, despite the fact that these processes are isostructural and isoelectronic.[28]

A review by Mayer highlights a number of recent reports demonstrating examples where hydrogen-atom transfer involves a proton-coupled-electron-transfer (PCET) mechanism.[29] For example, the reaction of a phenoxyl radical with phenol occurs by PCET;[30,31] a similar mechanism applies to the iminoxyl/oxime self-exchange reaction.[32] These mechanisms bear close similarity to the S_H2 mechanism proposed here; thus, in the phenol/phenoxyl system the proton is transferred to a lone pair on the oxygen atom in the phenoxyl radical and is thus assisted by hydrogen bonding.[31] In this sense, both PCET hydrogen-transfer reactions and S_H2 at boron are facilitated by acid–base interactions.

A related interaction was observed for radical ions, as in the mesolytic process,[33] where the hyperconjugation occurs between a π system to which has been removed or added an electron and an adjacent σ bond. The importance of the stereoelectronic effect of the side-chain deprotonation of alkyl aromatic radical cations has been investigated by Tolbert et al.[34] Evidence in favor of stereoelectronic control in C–C bond cleavage reactions of alkyl aromatic radical cations has been provided by Arnold et al. for a variety of systems.[35] These reactions can play an important role in synthetically useful processes.[36]

Conclusions

This study supports a new mechanism for attack of an oxygen radical center on an alkyl/aryl borane substrate. The model proposed suggests how the attack of the oxygen radical center, traditionally considered as a S_H2 reaction, involves instead nucleophilic-like attack of the oxygen lone

pair on the empty boron p orbital. The orientation of the incoming alkoxyl radical reflects the mechanism proposed, where the MOs involved align in a parallel way to maximize their overlap (Figure 2a,b). In order to achieve that, for any given orientation of the attacking group, the oxygen positions itself to have the lone pairs pointing toward the boron center, as in a nucleophilic substitution, and the methyl (in methoxyl) almost orthogonal to the leaving group. The single electron on the oxygen is not directly involved in the process, however, due to a stereoelectronic effect: the bond aligned with the SOMO orbital is deactivated and the corresponding ligand is prompted to leave as a radical species. From an energetic point of view, there are not significant differences in the attack of the methoxyl of *tert*-butoxyl radicals. The overall mechanism can be best described as a *nucleohomolytic* reaction.

Acknowledgments

We acknowledge the generous financial support of the Natural Sciences and Engineering Research Council (NSERC) and the Government of Ontario.

[1] G. E. Coates, K., Wade, *Organometallic Compounds*, Methuen and Co, New York, **1969**, vol. 1.
[2] J. J. Eisch, *The Chemistry of Organometallic Compounds*, MacMillam Co, New York, **1967**.
[3] K. U. Ingold, B. P. Roberts, *Free-Radical Substitution Reactions*, Wiley-Interscience, New York, **1971**, p. 245.
[4] A. G. Davies, D. Griller, B. P. Roberts, R. Tudor, *J. Chem. Soc. D* **1970**, 640; A. G. Davies, T. Maki, B. P. Roberts, *J. Chem. Soc. Perkin Trans. 2* **1972**, 744; P. J. Krusic, J. K. Kochi, *J. Am. Chem. Soc.* **1969**, *91*, 3942.
[5] A. G. Davies, K. U. Ingold, B. P. Roberts, R. Tudor, *J. Chem. Soc. B* **1971**, 698; A. G. Davies, B. P. Roberts, *J. Chem. Soc. B* **1971**, 1830; K. U. Ingold, *J. Chem. Soc. D* **1969**, 911.
[6] C. Ollivier, P. Renaud, *Chem. Rev.* **2001**, *101*, 3415.
[7] D. Griller, K. U. Ingold, L. K. Patterson, J. C. Scaiano, R. D. Small, *J. Am. Chem. Soc.* **1979**, *101*, 3780.
[8] M. J. Frisch, G. W. Trucks, H. B. Schlegel, G. E. Scuseria, M. A. Robb, J. R. Cheeseman, J. A. J. Montgomery, T. Vreven, K. N. Kudin, J. C. Burant, J. M. Millam, S. S. Iyengar, J. Tomasi, V. Barone, B. Mennucci, M. Cossi, G. Scalmani, N. Rega, G. A. Petersson, H. Nakatsuji, M. Hada, M. Ehara, K. Toyota, R. Fukuda, J. Hasegawa, M. Ishida, T. Nakajima, Y. Honda, O. Kitao, H. Nakai, M. Klene, X. Li, J. E. Knox, H. P. Hratchian, J. B. Cross, C. Adamo, J. Jaramillo, R. Gomperts, R. E. Stratmann, O. Yazyev, A. J. Austin, R. Cammi, C. Pomelli, J. W. Ochterski, P. Y. Ayala, K. Morokuma, G. A. Voth, P. Salvador, J. J. Dannenberg, V. G. Zakrzewski, S. Dapprich, A. D. Daniels, M. C. Strain, O. Farkas, D. K. Malick, A. D. Rabuck, K. Raghavachari, J. B. Foresman, J. V. Ortiz, Q. Cui, A. G. Baboul, S. Clifford, J. Cioslowski, B. B. Stefanov, G. Liu, A. Liashenko, P. Piskorz, I. Komaromi, R. L. Martin, D. J. Fox, T. Keith, M. A. Al-Laham, C. Y. Peng, A. Nanayakkara, M. Challacombe, P. M. W. Gill, B. Johnson, W. Chen, M. W. Wong, C. Gonzalez, J. A. Pople, *Gaussian 03*, Revision B.04, Gaussian, Inc., Pittsburgh, **2003**.
[9] C. Lee, W. Yang, R. G. Parr, *Physical Review B* **1988**, *37*, 785.
[10] K. Burke, J. P. Perdew, Y. Wang, *Electronic Density Functional Theory: Recent Progress and New Directions*, Plenum, **1998**.
[11] A. D. Becke, *J. Chem. Phys.* **1993**, *98*, 1372.
[12] C. Adamo, V. Barone, *J. Chem. Phys.* **1998**, *108*, 664.
[13] R. Ditchfield, W. J. Hehre, J. A. Pople, *J. Chem. Phys.* **1971**, *54*, 724.
[14] A. D. McLean, G. S. Chandler, *J. Chem. Phys.* **1980**, *72*, 5639.
[15] D. E. Woon, J. T. H. Dunning, *J. Chem. Phys.* **1993**, *98*, 1358.
[16] M. Head-Gordon, J. A. Pople, M. J. Frisch, *Chem. Phys. Lett.* **1988**, *153*, 503; M. Head-Gordon, T. Head-Gordon, *Chem. Phys. Lett.* **1994**, *220*, 112; M. J. Frisch, M. Head-Gordon, J. A. Pople, *Chem. Phys. Lett.* **1990**, *166*, 275; S. Saebo, J. Almlof, *Chem. Phys. Lett.* **1989**, *154*, 83.
[17] L. A. Curtiss, K. Raghavachari, G. W. Trucks, J. A. Pople, *J. Chem. Phys.* **1991**, *94*, 7221; L. A. Curtiss, J. E. Carpenter, K. Raghavachari, A. Pople, *J. Chem. Phys.* **1992**, *96*, 9030; L. A. Curtiss, P. C. Redfern, B. J. Smith, L. Radom, *J. Chem. Phys.* **1996**, *104*, 5148; L. A. Curtiss, K. Raghavachari, J. A. Pople, *J. Chem. Phys.* **1995**, *103*, 4192; L. A. Curtiss, K. Raghavachari, J. A. Pople, *J. Chem. Phys.* **1993**, *98*, 1293.
[18] L. A. Curtiss, P. C. Redfern, K. Raghavachari, V. Rassolov, J. A. Pople, *J. Chem. Phys.* **1999**, *110*, 4703; L. A. Curtiss, P. C. Redfern, K. Raghavachari, J. A. Pople, *J. Chem. Phys.* **2001**, *114*, 108; L. A. Curtiss, K. Raghavachari, P. C. Redfern, V. Rassolov, J. A. Pople, *J. Chem. Phys.* **1998**, *109*, 7764.
[19] G. A. DiLabio, D. A. Pratt, *J. Phys. Chem. A* **2000**, *104*, 1938; G. A. DiLabio, D. A. D. L. A. Pratt, J. S. Wright, *J. Phys. Chem. A* **1999**, *103*, 1653; J. S. Wright, D. J. Carpenter, D. J. McKay, K. U. Ingold, *J. Am. Chem. Soc.* **1997**, *119*, 4245; J. S. Wright, E. R. Johnson, G. A. DiLabio, *J. Am. Chem. Soc.* **2001**, *123*, 1173.
[20] A. E. Reed, L. A. Curtiss, F. Weinhold, *Chem. Rev.* **1988**, *88*, 899.
[21] J. E. Carpenter, F. Weinhold, *THEOCHEM* **1988**, *169*, 41; J. P. Foster, F. Weinhold, *J. Am. Chem. Soc.* **1980**, *102*, 7211.
[22] J. E. Carpenter, PhD Thesis, University of Wisconsin, Madison, WI, **1987**; F. Weinhold, J. E. Carpenter, *The Structure of Small Molecules and Ions*, Plenum, New York, **1988**, p. 227.
[23] P. Flükiger, H. P. Lüthi, S. Portmann, Weber, *J. Molekel 4.0*, Swiss National Supercomputing Centre CSCS, Manno, Switzerland, **2000**.
[24] R. G. Parr, *Density-Functional Theory of Atoms and Molecules*, Oxford University Press, New York, **1989**.
[25] V. Van Speybroeck, J. K. Van Cauter, B. Coussens, M. Waroquier, *Chemphyschem* **2005**, *6*, 180; B. J. Lynch, D. G. Truhlar, *J. Phys. Chem. A* **2001**, *105*, 2936; Y.-B. Fan, Z.-B. Ding, Q.-R. Wang, F.-G. Tao, *Chem. Phys. Lett.* **2000**, *328*, 39; B. S. Jursic, *J. Chem. Soc. Perkin Trans. 2* **1997**, 637; T. Hori, H. Takahashi, T. Nitta, *J. Chem. Phys.* DOI:10.1063/1.1611175; P. Hirva, M. Haukka, M. Jakonen, M. A. Moreno, *J. Mol. Modeling* **2008**, *14*, 171.
[26] D. A. Spiegel, K. B. Wiberg, L. N. Schacherer, M. R. Medeiros, J. L. Wood, *J. Am. Chem. Soc.* **2005**, *127*, 12513.
[27] M. v. Bochove, M. Swart, F. M. Bickelhaupt, *J. Am. Chem. Soc.* **2006**, *128*, 10738.
[28] A. P. Bento, F. M. Bickelhaupt, *J. Org. Chem.* **2007**, *72*, 2201.
[29] J. M. Mayer, *Annu. Rev. Phys. Chem.* **2004**, *55*, 363.
[30] G. Litwinienko, K. U. Ingold, *Acc. Chem. Res.* **2007**, *40*, 222.
[31] J. M. Mayer, D. A. Hrovat, J. L. Thomas, W. T. Borden, *J. Am. Chem. Soc.* **2002**, *124*, 11142.
[32] G. A. DiLabio, K. U. Ingold, *J. Am. Chem. Soc.* **2005**, *127*, 6693.
[33] C. Carra, F. Fiussello, G. Tonachini, *J. Org. Chem.* **1999**, *64*, 3867; P. Maslak, T. M. Vallombroso, W. J. Chapman Jr, J. N. Narvaez, *Angew. Chem. Int. Ed. Engl.* **1994**, *33*, 73.
[34] L. M. Tolbert, Z. Li, S. R. Sirimanne, D. G. VanDerveer, *J. Org. Chem.* **1997**, *62*, 3927.
[35] A. L. Perrott, D. R. Arnold, *Can. J. Chem.* **1992**, *70*, 272.
[36] M. Mella, M. Freccero, E. Fasani, A. Albini, *Chem. Soc. Rev.* **1998**, *27*, 81.

Received: February 17, 2008
Published Online: July 25, 2008

